

# Quantum Chemical Calculations of the $\text{Cl}^- + \text{CH}_3\text{I} \rightarrow \text{CH}_3\text{Cl} + \text{I}^-$ Potential Energy Surface<sup>†</sup>

Jiaxu Zhang,<sup>‡</sup> Upakarasamy Lourderaj,<sup>‡</sup> Srirangam V. Addepalli,<sup>§</sup> Wibe A. de Jong,<sup>⊥</sup> and William L. Hase<sup>\*,‡</sup>

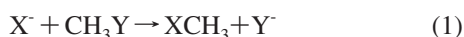
Department of Chemistry and Biochemistry, Texas Tech University, Lubbock, Texas 79409-106, High Performance Computing Center, Texas Tech University, Lubbock, Texas 79409, and Environmental Molecular Science Laboratory, Pacific Northwest National Laboratory, Richland, Washington 99352

Received: September 12, 2008; Revised Manuscript Received: November 3, 2008

Electronic structure theory calculations, using MP2 theory and the DFT functionals OPBE, OLYP, HCTH407, BhandH, and B97-1, were performed to characterize the structures, vibrational frequencies, and energies for stationary points on the  $\text{Cl}^- + \text{CH}_3\text{I} \rightarrow \text{ClCH}_3 + \text{I}^-$  potential energy surface. The aug-cc-pVDZ and aug-cc-pVTZ basis sets, with an effective core potential (ECP) for iodine, were employed. Single-point CCSD(T) calculations were performed to obtain the complete basis set (CBS) limit for the reaction energies. DFT was found to give significantly longer halide ion/carbon atom bond lengths for the ion–dipole complexes and central barrier transition state than MP2. BhandH, with either the aug-cc-pVDZ or aug-cc-pVTZ basis sets, gives good agreement with the experimental structures for both  $\text{CH}_3\text{I}$  and  $\text{CH}_3\text{Cl}$ . The frequencies of  $\text{CH}_3\text{I}$  and  $\text{CH}_3\text{Cl}$ , obtained with the different levels of theory and basis sets, are in excellent agreement with experiment. The major difference between the MP2 and DFT frequencies is for the imaginary frequency of the central barrier. Using the aug-cc-pVTZ basis the MP2 value for this frequency ranges from 1.26 to 1.59 times larger than those for the DFT functionals. Thus, the MP2 and DFT theories have different PES shapes in the vicinity of the  $[\text{Cl}^-\cdots\text{CH}_3\cdots\text{I}]^-$  central barrier. The CCSD(T)/CBS energies are in good agreement with experiments for the complexation energies and reaction exothermicity, with a small 1 kcal/mol difference for the latter. The CCSD(T)/CBS central barrier height is lower than values deduced by using statistical theoretical models to fit the  $\text{Cl}^- + \text{CH}_3\text{I} \rightarrow \text{ClCH}_3 + \text{I}^-$  experimental rate constant, which is consistent with the expected nonstatistical dynamics for the reaction. The BhandH energies are in overall best agreement with the CCSD(T) values, with a largest difference of only 0.7 kcal/mol.

## I. Introduction

There is considerable interest in understanding the atomic-level dynamics of gas-phase bimolecular nucleophilic substitution ( $\text{S}_{\text{N}}2$ ) reactions of the type<sup>1–10</sup>



These reactions are of central importance in gas-phase ion chemistry and organic reaction mechanisms.<sup>11</sup> Studies of these reactions in the gas phase have provided the opportunity to probe the intrinsic reaction mechanism without solvent,<sup>12</sup> and it is well-known that the reactions proceed via a double-well potential. The two wells correspond to loose ion–dipole complexes, i.e., the pre- and postreaction complexes  $\text{X}^-\cdots\text{CH}_3\text{Y}$  and  $\text{XCH}_3\cdots\text{Y}^-$ , which are separated by a  $[\text{X}^-\cdots\text{CH}_3\cdots\text{Y}]^-$  central barrier. The energy profile for the  $\text{Cl}^- + \text{CH}_3\text{I} \rightarrow \text{ClCH}_3 + \text{I}^-$  reaction is shown in Figure 1. This potential model has been confirmed by numerous theoretical and experimental studies,<sup>13–16</sup> including a structural characterization of a  $\text{S}_{\text{N}}2$  ion–dipole complex.<sup>17,18</sup>

For the first proposed mechanism of the gas-phase  $\text{X}^- + \text{CH}_3\text{Y}$  reaction, it is assumed that the reaction system becomes trapped in the  $\text{X}^-\cdots\text{CH}_3\text{Y}$  and  $\text{XCH}_3\cdots\text{Y}^-$  complexes with

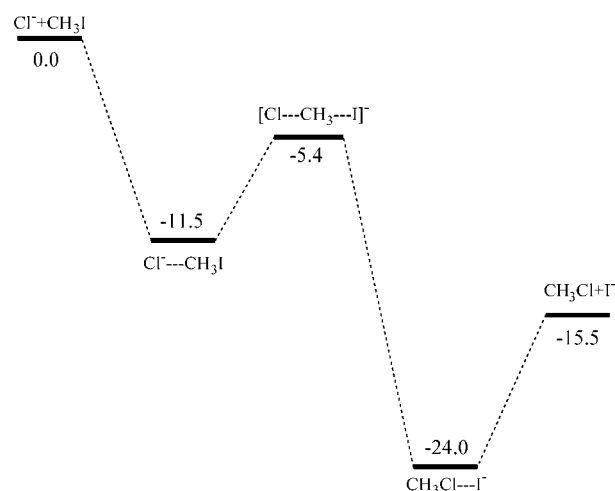


**Figure 1.** Schematic energy profile for the  $\text{Cl}^- + \text{CH}_3\text{I} \rightarrow \text{ClCH}_3 + \text{I}^-$  reaction at the CCSD(T)/CBS level of theory. The energies shown are in kcal/mol and are relative to the  $\text{Cl}^- + \text{CH}_3\text{I}$  reactants. Zero-point energies are not included.

complete randomization of their vibrational energies.<sup>2</sup> An ion–molecule capture theoretical model, such as classical trajectories<sup>19</sup> or variational transition state,<sup>20</sup> is used to calculate the  $\text{X}^- + \text{CH}_3\text{Y} \rightarrow \text{X}^-\cdots\text{CH}_3\text{Y}$  association rate constant and RRKM theory is used to calculate the unimolecular lifetime of each complex and the branching ratio for its two unimolecular

<sup>†</sup> Part of the “Max Wolfsberg Festschrift”.

\* Corresponding author. E-mail bill.hase@ttu.edu.

<sup>‡</sup> Department of Chemistry and Biochemistry, Texas Tech University.

<sup>§</sup> High Performance Computing Center, Texas Tech University.

<sup>⊥</sup> Environmental Molecular Science Laboratory, Pacific Northwest National Laboratory.

pathways,<sup>21</sup> e.g.,  $\text{X}^{\cdots}\text{CH}_3\text{Y} \rightarrow \text{X}^- + \text{CH}_3\text{Y}$  and  $\text{X}^{\cdots}\text{CH}_3\text{Y} \rightarrow \text{XCH}_3\text{---Y}^-$ . This model predicts that if one of the transition states (TSs), i.e., the one at the central barrier or either the  $\text{X}^- + \text{CH}_3\text{Y}$  or  $\text{XCH}_3 + \text{Y}^-$  variational TS, has a sum of states (or free energy) much smaller than those of the other two, the  $\text{S}_{\text{N}}2$  rate constant is determined by properties of this TS and given by transition state theory.<sup>22</sup>

Both experimental<sup>23–31</sup> and computational<sup>32–44</sup> studies have shown that this model mechanism does not characterize all  $\text{X}^- + \text{CH}_3\text{Y}$   $\text{S}_{\text{N}}2$  reactions. Due to inefficient energy transfer between  $\text{X}^- + \text{CH}_3\text{Y}$  relative translation and  $\text{CH}_3\text{Y}$  rotation and vibration, the  $\text{X}^- + \text{CH}_3\text{Y} \rightarrow \text{X}^{\cdots}\text{CH}_3\text{Y}$  association rate constant may be smaller than that of the capture model.<sup>34,36</sup> Energy randomization may be incomplete for the  $\text{X}^{\cdots}\text{CH}_3\text{Y}$  prereaction complex<sup>24,26,29,30,33,34,37–39</sup> and for a highly exothermic  $\text{S}_{\text{N}}2$  reaction the reaction system may move directly from the  $[\text{X}^{\cdots}\text{CH}_3\text{---Y}]^-$  central barrier to products without forming the  $\text{XCH}_3\text{---Y}^-$  postreaction complex.<sup>31,43,44</sup> Upon C–Y stretch vibrational or  $\text{X}^- + \text{CH}_3\text{Y}$  translational activation, the mechanism may become direct without forming either the  $\text{X}^{\cdots}\text{CH}_3\text{Y}$  or  $\text{XCH}_3\text{---Y}^-$  complex.<sup>27,28,32,34,40,41,43,44</sup> In chemical dynamics simulations of the  $\text{Cl}^- + \text{CH}_3\text{Cl}$  and  $\text{Cl}^- + \text{CH}_3\text{Br}$   $\text{S}_{\text{N}}2$  reactions extensive recrossings of the central barrier are observed<sup>35,37,42</sup> in contrast to the prediction of RRKM theory that there should be negligible recrossings. Quantum dynamics calculations are in agreement with the above results, and illustrate the important role of resonances in  $\text{S}_{\text{N}}2$  reactions.<sup>45–50</sup>

Interpreting the dynamics and kinetics of  $\text{S}_{\text{N}}2$  reactions, by either theoretical calculations or chemical dynamics simulations,<sup>51,52</sup> requires accurate potential energy surfaces (PES's). G2(+) theory has been used to calculate energetics for the reactions  $\text{X}^- + \text{CH}_3\text{X} \rightarrow \text{XCH}_3 + \text{X}^-$  and  $\text{X}^- + \text{CH}_3\text{Y} \rightarrow \text{XCH}_3 + \text{Y}^-$ , X, Y = F, Cl, Br, and I.<sup>53–55</sup> Density functional theory (DFT) and ab initio methods have been compared for calculating  $\text{X}^- + \text{CH}_3\text{X} \rightarrow \text{XCH}_3 + \text{X}^-$  (X = F, Cl, Br, I) PESs.<sup>56–58</sup> A range of DFT methods have been compared for  $\text{X}^- + \text{CH}_3\text{Y} \rightarrow \text{XCH}_3 + \text{Y}^-$  (X, Y = F, Cl, Br)  $\text{S}_{\text{N}}2$  reactions.<sup>59</sup> DFT models have been assessed for the  $\text{CH}_3\text{X} + \text{F}^-$  (X = F, Cl, CN, OH, SH, NH<sub>2</sub>, PH<sub>2</sub>) reactions<sup>60</sup> and a range of ab initio and DFT methods have been used to analyze the  $\text{X}^- + \text{CH}_3\text{X}$  (X = F, Cl, CN, OH, SH, NH<sub>2</sub>, PH<sub>2</sub>)  $\text{S}_{\text{N}}2$  reactions.<sup>61</sup> Recently, Bickelhaupt and co-workers carried out a detailed evaluation of the performance of many DFT functionals for describing PES's of a wide range of  $\text{S}_{\text{N}}2$  reactions.<sup>62</sup> Analytics PES's and ab initio PES's for direct dynamics have been used in studies of the  $\text{Cl}^- + \text{CH}_3\text{Cl}$ ,<sup>35,42,63–65</sup>  $\text{Cl}^- + \text{CH}_3\text{Br}$ ,<sup>38,66</sup>  $\text{F}^- + \text{CH}_3\text{Cl}$ ,<sup>41,67</sup>  $\text{F}^- + \text{CH}_3\text{OH}$ ,<sup>43</sup> and  $\text{Cl}^- + \text{CH}_3\text{I}$   $\text{S}_{\text{N}}2$  reactions. High-level CCSD(T) ab initio calculations have provided properties for the  $\text{F}^- + \text{CH}_3\text{Cl}$ ,<sup>67,68</sup>  $\text{F}^- + \text{CH}_3\text{F}$ ,<sup>69</sup>  $\text{Cl}^- + \text{CH}_3\text{Cl}$ ,<sup>70</sup>  $\text{X}^- + \text{CH}_3\text{Y} \rightarrow \text{XCH}_3 + \text{Y}^-$  (X, Y = F, Cl, Br),<sup>59</sup>  $\text{CH}_3\text{X} + \text{F}^-$  (X = F, Cl, CN, OH, SH, NH<sub>2</sub>, PH<sub>2</sub>),<sup>60</sup>  $\text{OH}^- + \text{CH}_{(4-n)}\text{Cl}_n$  ( $n = 1–4$ ),<sup>71</sup> and  $\text{CH}_3\text{X} + \text{X}^-$  (X = F, Cl, CN, OH, SH, NH<sub>2</sub>, PH<sub>2</sub>)  $\text{S}_{\text{N}}2$  reactions.<sup>61</sup>

In recent work a direct chemical dynamics simulation,<sup>31</sup> at the MP2(fc)/ECP/aug-cc-pVDZ level of theory, was used to study the dynamics of the  $\text{Cl}^- + \text{CH}_3\text{I}$   $\text{S}_{\text{N}}2$  reaction and compare with results of ion imaging experiments. To investigate the adequacy of these MP2 direct dynamics, it is of interest to compare properties of the  $\text{Cl}^- + \text{CH}_3\text{I} \rightarrow \text{ClCH}_3 + \text{I}^-$  PES, given by the above MP2 method and other electronic structure theoretical methods. In the work presented here, stationary point properties of the  $\text{Cl}^- + \text{CH}_3\text{I}$   $\text{S}_{\text{N}}2$  reaction are calculated by using the DFT, MP2, and CCSD(T) theories with different basis sets and DFT functionals. Comparisons are made between the

results of these calculations and with experimental and previously obtained theoretical results.

## II. Computational Procedure

All calculations were carried out with the NWChem program.<sup>72</sup> MP2<sup>73,74</sup> and DFT,<sup>62,75–78</sup> with the OPBE, OLYP, HCTH407, BhandH, and B97-1 functionals, were used to calculate the energies, geometries, and frequencies of the stationary points for the reactants, ion–dipole complexes, transition state, and products on the  $\text{Cl}^- + \text{CH}_3\text{I} \rightarrow \text{ClCH}_3 + \text{I}^-$  PES. Three different basis sets were employed for the calculations. For the ECP/6-31+G(d) basis, the 6-31+G(d) basis<sup>79</sup> was used for the C, H, and Cl atoms and, for iodine, the Wadt and Hay effective core potential (ECP) was used for the core electrons and an uncontracted 3s3p basis set for the valence electrons.<sup>80</sup> This iodine basis set was augmented by a d-polarization function with a 0.262 exponent, and s, p, and d diffuse functions with exponents of 0.034, 0.039, and 0.0873, respectively.<sup>81</sup> For the basis sets identified as ECP/d and ECP/t, the double- (d) and triple- $\zeta$  (t) basis sets, aug-cc-pVDZ and aug-cc-pVTZ,<sup>82</sup> were used for the C, H, and Cl atoms. In addition, for the ECP/t basis the above iodine basis was further augmented by an f-polarization function with a 0.52 exponent.<sup>83</sup>

Structures, frequencies, and energies were calculated at the MP2 level of theory with each of the above three basis sets and at the DFT level of theory with only the ECP/d and ECP/t basis sets. The frozen core (fc) orbital method was used for MP2 calculations. The stationary nature of structures was confirmed by harmonic vibrational frequency calculations, that is, the potential minima possess all real frequencies, whereas the transition state possesses only one imaginary frequency. The harmonic zero-point energy (ZPE) was obtained at all these levels of theory.

To obtain more reliable energies, higher level single-point energy calculations were performed at the CCSD(T) level of theory.<sup>84</sup> The frozen core (fc) orbital method was used, as for the above MP2 calculations. The calculations were performed with the correlation consistent Gaussian basis sets, as above, denoted by aug-cc-pVXZ, where X is the cardinal number for the basis set (X = D, T, Q, and 5).<sup>82</sup> The results were extrapolated to the complete basis set (CBS) limit.<sup>85</sup> For the C, H, and Cl atoms the aug-cc-pVXZ basis was used. For iodine the Peterson aug-cc-pVXZ basis, with a pseudopotential (PP),<sup>86</sup> was used. Only the 5s5p orbitals were correlated for I, which is consistent with the correlation for other atoms, i.e. 2s2p for C, 3s3p for Cl, and 1s for H. Following the terminology used above, for the MP2 and DFT calculations, these basis sets are identified as PP/x, where x = d, t, q, and 5. These CCSD(T) calculations are based on MP2/PP/d minimum geometries, which are very close to MP2/ECP/d geometry. The largest differences between these two geometries are 0.023 Å for the C---I bond of the  $\text{ClCH}_3\text{---I}^-$  complex and 0.28° for the I–C–H and Cl–C–H angles of the transition state.

## III. Results and Discussion

The geometries, harmonic vibrational frequencies, and relative energies determined from the electronic structure calculations are discussed in the following, and summarized in Tables 1–4 and Figures 1 and 2.

**A. Geometries.** The stationary point geometries are listed in Table 1 and depicted in Figure 2. The MP2 and MP2(fc) geometries are quite similar, with the bond distance and angle deviations less than 0.023 Å and 0.14°, respectively, illustrating

**TABLE 1: Geometries of Stationary Points for the  $\text{Cl}^- + \text{CH}_3\text{I} \rightarrow \text{CH}_3\text{Cl} + \text{I}^-$  Reaction<sup>a</sup>**

	$R_{\text{C-Cl}}$	$R_{\text{C-I}}$	$R_{\text{C-H}}$	$\angle\text{I-C-H}$	$\angle\text{Cl-C-H}$	$\angle\text{H-C-H}$
Cl <sup>-</sup> + CH <sub>3</sub> I reactants						
MP2		2.143 <sup>b</sup> (2.145) <sup>d</sup>	1.094(1.096)	107.98(107.97)		110.91(110.92)
		2.115 <sup>c</sup> (2.117)	1.079(1.083)	107.87(107.89)		111.02(111.00)
OPBE		2.139	1.097	107.85		111.05
		2.124	1.091	107.84		111.06
OLYP		2.158	1.096	107.79		111.10
		2.143	1.089	107.72		111.16
BhandH		2.140	1.093	107.84		111.05
		2.126	1.084	107.88		111.01
HCTH407		2.155	1.093	107.72		111.16
		2.140	1.086	107.66		111.22
B97-1		2.147	1.095	108.00		110.90
		2.133	1.086	107.83		111.06
expt <sup>e</sup>		2.132	1.084	107.7		111.2
Cl <sup>-</sup> ---CH <sub>3</sub> I complex						
MP2	3.068(3.091)	2.186 (2.185)	1.090(1.092)	107.43(107.55)	72.45(72.48)	111.44(111.32)
	3.047(3.068)	2.149 (2.151)	1.076(1.080)	107.72(107.77)	72.12(72.08)	111.17(111.12)
OPBE	3.234	2.196	1.093	107.24	72.76	111.61
	3.267	2.172	1.087	107.43	72.57	111.44
OLYP	3.239	2.228	1.092	106.79	73.21	112.01
	3.282	2.199	1.085	107.00	73.00	111.83
BhandH	3.092	2.193	1.089	107.28	72.72	111.57
	3.107	2.170	1.081	107.54	72.46	111.33
HCTH407	3.176	2.223	1.089	106.81	73.19	112.00
	3.213	2.196	1.082	107.07	72.93	111.76
B97-1	3.061	2.229	1.090	106.69	73.31	112.11
	3.080	2.198	1.082	107.00	73.00	111.82
[Cl---CH <sub>3</sub> --I] <sup>-</sup> saddle point						
MP2	2.383(2.384)	2.582 (2.588)	1.081(1.082)	92.20(92.10)	87.80(87.90)	119.85(119.87)
	2.326(2.327)	2.554 (2.559)	1.067(1.070)	91.61(91.47)	88.39(88.53)	119.92(119.93)
OPBE	2.426	2.574	1.085	93.26	86.74	119.68
	2.398	2.557	1.079	92.82	87.18	119.76
OLYP	2.476	2.632	1.083	92.92	87.08	119.74
	2.444	2.621	1.076	92.44	87.56	119.82
BhandH	2.449	2.584	1.080	93.41	86.59	119.65
	2.425	2.577	1.071	93.02	86.98	119.72
HCTH407	2.483	2.633	1.081	93.03	86.97	119.72
	2.444	2.628	1.073	92.31	87.69	119.84
B97-1	2.462	2.603	1.082	93.33	86.67	119.67
	2.436	2.595	1.073	92.89	87.11	119.75
ClCH <sub>3</sub> ---I <sup>-</sup> complex						
MP2	1.824(1.827)	3.535 (3.540)	1.091(1.093)	71.90(71.76)	108.26(108.30)	110.64(110.62)
	1.802(1.808)	3.491 (3.491)	1.077(1.081)	71.48(71.50)	108.52(108.44)	110.40(110.49)
OPBE	1.801	4.017	1.095	71.34	108.68	110.24
	1.793	4.062	1.090	71.25	108.79	110.15
OLYP	1.830	3.954	1.094	71.78	108.23	110.68
	1.820	4.006	1.088	71.67	108.33	110.59
BhandH	1.816	3.653	1.091	71.66	108.37	110.55
	1.805	3.669	1.083	71.42	108.57	110.36
HCTH407	1.816	3.838	1.092	71.30	108.58	110.35
	1.806	3.874	1.086	71.38	108.62	110.31
B97-1	1.848	3.613	1.092	72.21	107.80	111.08
	1.836	3.631	1.084	72.22	107.96	110.92
ClCH <sub>3</sub> + I <sup>-</sup> products						
MP2	1.794(1.797)		1.094(1.096)		108.29(108.27)	110.63(110.64)
	1.774(1.780)		1.080(1.084)		108.39(108.36)	110.53(110.57)
OPBE	1.778		1.098		108.63	110.30
	1.771		1.093		108.73	110.21
OLYP	1.800		1.097		108.35	110.57
	1.794		1.091		108.37	110.55
BhandH	1.787		1.094		108.32	110.60
	1.777		1.086		108.50	110.43
HCTH407	1.785		1.095		108.58	110.35
	1.778		1.088		108.66	110.27
B97-1	1.810		1.095		107.97	110.93
	1.800		1.087		108.13	110.78
expt <sup>e</sup>	1.785		1.090		108.1	110.8

<sup>a</sup> Bond lengths are in angstroms (Å), and angles are in deg. <sup>b</sup> Upper values are calculated with the ECP/d basis set. <sup>c</sup> Lower values are calculated with the ECP/t basis set. <sup>d</sup> Values in parentheses are calculated at the MP2 theory with the frozen core orbital method (fc). <sup>e</sup> The experimental geometries of CH<sub>3</sub>I and CH<sub>3</sub>Cl are from ref 87.

the accuracy of the frozen core (fc) approximation. For the MP2 and different DFT functionals the structures given by the ECP/d and ECP/t basis sets are similar. However, the latter gives shorter bond lengths for each of the stationary points, except for the

Cl<sup>-</sup>---C and C---I<sup>-</sup> bonds of the complexes. For these bonds, ECP/d gives shorter bond lengths when used with DFT. The difference in the ECP/d and ECP/t values for the carbon-halogen bond lengths is largest and 0.052 Å for the C---I<sup>-</sup> bond of

**TABLE 2: Harmonic Frequencies of Stationary Points for the  $\text{Cl}^- + \text{CH}_3\text{I} \rightarrow \text{CH}_3\text{Cl} + \text{I}^-$  Reaction<sup>a</sup>**

mode	MP2	OPBE	OLYP	BhandH	HCTH407	B97-1	expt <sup>e</sup>
			$\text{CH}_3\text{I}$				
A <sub>1</sub> C–I str	551 <sup>c</sup> (550) 579 <sup>b</sup> (576) <sup>d</sup>	543 557	517 530	549 564	529 540	516 532	539
E CH <sub>3</sub> rock	910(907) 924(917)	870 875	870 878	910 919	876 883	887 897	901
A <sub>1</sub> CH <sub>3</sub> deform	1290(1285) 1318(1305)	1219 1238	1223 1249	1285 1309	1229 1253	1256 1282	1276
E CH <sub>3</sub> deform	1469(1461) 1495(1492)	1391 1419	1398 1433	1456 1488	1402 1436	1429 1467	1465
A <sub>1</sub> C–H str	3112(3106) 3166(3116)	3052 3048	3046 3042	3121 3177	3071 3065	3072 3070	3080
E C–H str	3238(3230) 3249(3236)	3189 3169	3172 3153	3245 3230	3203 3182	3191 3177	3188
			$\text{CH}_3\text{Cl}$				
A <sub>1</sub> C–Cl str	754(752) 776(767)	755 756	714 714	760 764	726 728	724 726	740
E CH <sub>3</sub> rock	1033(1031) 1058(1047)	990 1004	989 1005	1035 1054	999 1015	1003 1022	1038
A <sub>1</sub> CH <sub>3</sub> deform	1371(1370) 1413(1397)	1309 1334	1312 1340	1374 1402	1323 1351	1334 1367	1383
E CH <sub>3</sub> deform	1483(1477) 1516(1508)	1408 1434	1412 1445	1471 1503	1417 1450	1441 1478	1482
A <sub>1</sub> C–H str	3110(3104) 3166(3112)	3037 3029	3030 3025	3112 3106	3052 3044	3066 3060	3074
E C–H str	3229(3223) 3242(3225)	3160 3137	3145 3126	3226 3210	3170 3147	3179 3162	3166
			$\text{Cl}^{\cdots}\text{---CH}_3\text{I}$				
E Cl <sup>-</sup> bend	70(65) 66(58)	55 48	57 50	65 65	62 58	73 72	
A <sub>1</sub> Cl–C str	103(100) 101(98)	65 58	71 65	97 95	82 77	99 93	
A <sub>1</sub> C–I str	473(474) 505(505)	424 449	386 414	439 465	396 424	360 393	
E CH <sub>3</sub> rock	881(875) 895(884)	817 824	818 829	872 884	822 834	836 857	
A <sub>1</sub> CH <sub>3</sub> deform	1218(1222) 1263(1244)	1157 1179	1153 1190	1216 1243	1153 1192	1169 1206	
E CH <sub>3</sub> deform	1444(1435) 1471(1467)	1370 1401	1378 1416	1430 1466	1379 1417	1400 1443	
A <sub>1</sub> C–H str	3149(3142) 3201(3150)	3089 3084	3084 3080	3161 3157	3105 3100	3115 3111	
E C–H str	3290(3281) 3301(3282)	3241 3219	3232 3210	3304 3286	3257 3236	3257 3238	
			$[\text{Cl}^{\cdots}\text{---CH}_3\text{---I}]^-$				
E Cl–C–I bend	178(175) 187(184)	164 170	153 158	167 162	152 157	159 165	
A <sub>1</sub> Cl–C–I str	171(170) 179(179)	150 155	139 143	160 173	138 141	154 156	
E CH <sub>3</sub> rock	921(914) 951(948)	841 864	812 834	881 903	811 832	845 865	
A <sub>2</sub> out-of-plane bend	1023(986) 983(987)	903 912	910 916	1012 1016	916 921	954 962	
E CH <sub>3</sub> deform	1440(1404) 1427(1424)	1330 1349	1346 1371	1396 1419	1348 1373	1371 1400	
A <sub>1</sub> C–H str	3216(3206) 3266(3217)	3141 3143	3143 3144	3224 3225	3164 3163	3173 3176	
E C–H str	3426(3419) 3441(3421)	3360 3345	3355 3342	3437 3427	3379 3364	3381 3371	
reaction coordinate	437 <i>i</i> (450 <i>i</i> ) 489 <i>i</i> (481 <i>i</i> )	317 <i>i</i> 330 <i>i</i>	292 <i>i</i> 307 <i>i</i>	367 <i>i</i> 388 <i>i</i>	293 <i>i</i> 315 <i>i</i>	309 <i>i</i> 329 <i>i</i>	
			$\text{ClCH}_3\text{---I}^-$				
E I <sup>-</sup> bend	74(71) 60(59)	42 37	45 36	62 62	53 44	63 50	
A <sub>1</sub> C–I str	74(74) 74(73)	46 41	49 41	64 63	87 51	70 66	
A <sub>1</sub> Cl–C str	677(674) 701(690)	688 696	631 641	679 688	637 646	624 631	
E CH <sub>3</sub> rock	1003(999) 1021(1010)	965 977	959 975	1003 1024	982 981	968 984	
A <sub>1</sub> CH <sub>3</sub> deform	1318(1320) 1361(1344)	1289 1312	1289 1318	1334 1363	1294 1319	1289 1316	
E CH <sub>3</sub> deform	1465(1458) 1490(1484)	1401 1427	1404 1438	1455 1489	1406 1439	1424 1462	
A <sub>1</sub> C–H str	3139(3133) 3187(3139)	3066 3057	3060 3054	3142 3136	3080 3072	3098 3091	
E C–H str	3272(3264) 3282(3265)	3200 3175	3190 3167	3269 3250	3210 3188	3227 3206	

<sup>a</sup> Frequencies are in units of  $\text{cm}^{-1}$ . <sup>b</sup> Upper values are calculated with the ECP/d basis set. <sup>c</sup> Lower values are calculated with the ECP/t basis set. <sup>d</sup> Values in parentheses are calculated with MP2 theory and the frozen core orbital method (fc). <sup>e</sup> The experimental harmonic frequencies of  $\text{CH}_3\text{I}$  and  $\text{CH}_3\text{Cl}$  are from ref 88.

**TABLE 3: Electronic Structure Theory Energies for  $\text{Cl}^- + \text{CH}_3\text{I} \rightarrow \text{CH}_3\text{Cl} + \text{I}^-$  Stationary Points<sup>a</sup>**

theory	stationary points			
	$\text{Cl}^- \cdots \text{CH}_3\text{I}$	$[\text{Cl}-\text{CH}_3-\text{I}]^-$	$\text{I}^- \cdots \text{CH}_3\text{Cl}$	$\text{I}^- + \text{CH}_3\text{Cl}$
MP2/ECP/6-31+G(d)	-10.7 (-10.7) <sup>b</sup>	-4.6 (-4.6)	-28.6 (-28.5)	-20.9 (-20.8)
MP2	-12.1 (-11.6) <sup>c</sup>	-4.9 (-4.0)	-22.4 (-21.6)	-13.0 (-12.2)
	-11.5 (-11.2) <sup>d</sup>	-2.6 (-2.1)	-20.5 (-19.2)	-10.5 (-9.2)
OPBE	-8.8	-4.8	-20.1	-14.3
	-8.1	-3.6	-19.0	-13.3
OLYP	-9.2	-5.5	-18.9	-12.6
	-8.5	-4.0	-17.6	-11.5
BhandH	-11.3	-6.4	-24.6	-16.3
	-10.8	-4.7	-23.7	-15.8
HCTH407	-11.4	-7.6	-21.7	-13.8
	-10.7	-5.8	-20.1	-12.3
B97-1	-11.5	-8.5	-21.6	-12.8
	-11.0	-7.0	-20.6	-12.2
CCSD(T)/CBS	-11.5	-5.4	-24.0	-15.5
	$[-11.4]^e$	$[-5.2]$	$[-23.1]$	$[-14.7]$

<sup>a</sup> Energies (kcal/mol) are with respect to the  $\text{Cl}^- + \text{CH}_3\text{I}$  reactants and do not include zero-point energy (ZPE). <sup>b</sup> Values in parentheses are calculated with MP2 theory and the frozen core (fc) orbital method. <sup>c</sup> Upper values are calculated with the ECP/d basis set. <sup>d</sup> Lower values are calculated with the ECP/t basis set. <sup>e</sup> Values in square brackets include ZPE, with ZPE calculated at the MP2/PP/d level of theory (see the text). The frozen core (fc) orbital method was used for the CCSD(T) calculations.

**TABLE 4: CCSD(T)/CBS Energies for  $\text{Cl}^- + \text{CH}_3\text{I} \rightarrow \text{CH}_3\text{Cl} + \text{I}^-$  Stationary Points and Comparison with Experimental and Previous Theoretical Values<sup>a</sup>**

theory	stationary point			
	$\text{Cl}^- \cdots \text{CH}_3\text{I}$	$[\text{Cl}-\text{CH}_3-\text{I}]^-$	$\text{I}^- \cdots \text{CH}_3\text{Cl}$	$\text{I}^- + \text{CH}_3\text{Cl}$
CCSD(T)/PP/d <sup>b</sup>	-11.7	-5.8	-21.4	-12.2
CCSD(T)/PP/t	-11.4	-4.9	-22.1	-13.3
CCSD(T)/PP/q	-11.5	-5.2	-23.2	-14.6
CCSD(T)/PP/5	-11.5	-5.3	-23.7	-15.2
CCSD(T)/CBS	-11.5	-5.4	-24.0	-15.5
	$[-11.4]$	$[-5.2]$	$[-23.1]$	$[-14.7]$
G2(+) <sup>c</sup>		-3.4		
	$[-10.9]$	$[-3.3]$	$[-20.2]$	$[-11.9]$
MP2/PTZ+d <sup>d</sup>		-2.7		-13.5
		$[-2.7]$		$[-12.7]$
expt		-2.7 <sup>e</sup>		-14.5 <sup>g</sup>
		$[-4.6]^f$		$[-13.7]^g$

<sup>a</sup> Energies (kcal/mol) are with respect to the reactants  $\text{Cl}^- + \text{CH}_3\text{I}$  and do not include zero-point energy (ZPE). The values in square brackets include ZPE, with ZPE calculated at the MP2/PP/d level of theory (see the text). The frozen core (fc) orbital method was used for the CCSD(T) calculations. <sup>b</sup> For the PP/x basis sets, x = d, t, q, and 5, the aug-cc-pVXZ (X = D, T, Q, and 5) basis set was used for the C, H, and Cl atoms and the aug-cc-pVXZ basis with a pseudopotential (PP) was used for iodine. <sup>c</sup> From ref 54. <sup>d</sup> From ref 83. <sup>e</sup> Classical barrier height obtained by fitting the experimental rate constant with TST; from ref 83. <sup>f</sup> The 0 K barrier, with ZPE included, obtained by fitting the reaction rate constant with an ion-molecule capture statistical model; from ref 25. <sup>g</sup> The reaction exothermicity at 0 K without ZPE calculated from standard molar enthalpies of formation in ref 90 and harmonic frequency data in ref 88. The values in square brackets include ZPE.

$\text{ClCH}_3 \cdots \text{I}^-$  with DFT/OLYP theory, and smallest and 0.024 Å for the Cl-C bond of  $[\text{Cl}-\text{CH}_3-\text{I}]^-$  with DFT/BhandH theory.

DFT gives significantly longer  $\text{Cl}^- \cdots \text{C}$  and  $\text{C} \cdots \text{I}^-$  bonds for the complexes, and longer Cl-C and C-I bonds for the TS, than does MP2. For the  $\text{Cl}^- \cdots \text{CH}_3\text{I}$  and  $\text{ClCH}_3 \cdots \text{I}^-$  complexes, the hybrid functionals (B97-1 and BhandH) appear to give better geometries than the GGA functionals (OPBE, OLYP, HCTH), when compared with MP2 geometries. The largest difference in the geometries given by MP2 theory and the different functionals of DFT is for the  $\text{C} \cdots \text{I}^-$  bond length of the  $\text{ClCH}_3 \cdots \text{I}^-$  postreaction complex. The DFT functionals give larger values for this bond length and, using the ECP/d basis set, the smallest

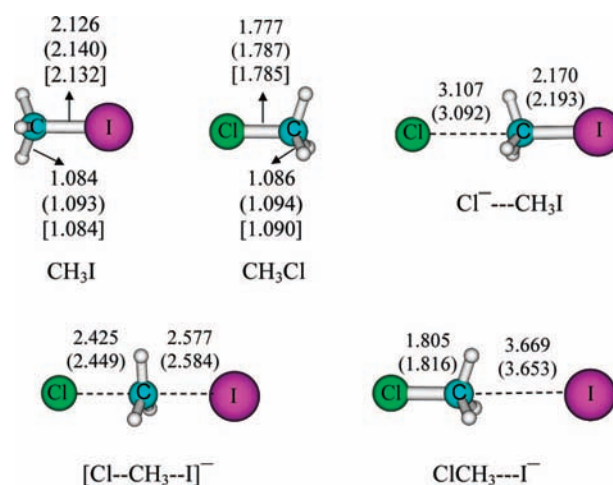


**Figure 2.** Geometries of stationary points for the  $\text{Cl}^- + \text{CH}_3\text{I} \rightarrow \text{ClCH}_3 + \text{I}^-$  reaction optimized at the BhandH level of theory, and comparison with experiment.<sup>87</sup> Bond lengths are in Å. The ECP/t values are not enclosed in parentheses and brackets. The ECP/d and experimental values are enclosed in parentheses and brackets, respectively.

and largest differences with MP2 are 0.078 and 0.482 Å for the B97-1 and OPBE functionals, respectively. For the ECP/t basis, the B97-1 and OPBE functionals still give the smallest and largest differences with MP2, which are 0.140 and 0.571 Å, respectively.

As shown in Table 1, the accuracy of the structures calculated for the  $\text{CH}_3\text{I}$  reactant and  $\text{CH}_3\text{Cl}$  product, in comparison with experiment,<sup>87</sup> depends on the level of theory and basis set. Of the methods considered here, BhandH with either the ECP/d or ECP/t basis set gives the best agreement with the experimental structures when considering both  $\text{CH}_3\text{I}$  and  $\text{CH}_3\text{Cl}$ . The BhandH structures, and their comparison with experiment, are summarized in Figure 2.

It is of interest to consider some of the specific differences of the  $\text{CH}_3\text{I}$  and  $\text{CH}_3\text{Cl}$  structures calculated by different basis sets. As discussed above, the ECP/t basis gives shorter C-H, C-I, and C-Cl bond lengths. The ECP/d and ECP/t basis sets give values for the C-H bond length of  $\text{CH}_3\text{I}$  whose difference ranges from 0.015 Å for MP2 to 0.006 Å for DFT/OPBE. The difference in the ECP/d and ECP/t values for the C-H bond length of  $\text{CH}_3\text{Cl}$  ranges from 0.014 Å for MP2 to 0.005 Å for

DFT/OPBE. The differences in the ECP/d and ECP/t bond lengths are even larger for the C–I and C–Cl bond lengths of  $\text{CH}_3\text{I}$  and  $\text{CH}_3\text{Cl}$ . For the C–I bond, the difference in the ECP/d and ECP/t bond lengths varies from 0.028 Å for MP2 to 0.014 Å for BhandH and B97-1. For the C–Cl bond length, this difference varies from 0.020 Å for MP2 to 0.006 Å for OLYP. When used with MP2 theory, the ECP/d and ECP/t basis sets give larger differences in the C–H, C–I, and C–Cl bond lengths than when used with the different DFT functionals. The bond angles of  $\text{CH}_3\text{I}$  and  $\text{CH}_3\text{Cl}$  are less sensitive to the basis set than are the bond lengths.

The geometries of the pre- and postreaction complexes and transition state have been previously calculated at the G2(+) level.<sup>54</sup> The structures obtained by our calculations are consistent with those determined from the G2(+) level with bond angle differences 1.1° or less. The major structural difference lies in the C---I bond length of the postreaction  $\text{ClCH}_3\text{---I}^-$  complex. The G2(+) value for this bond length is 3.741 Å. The BhandH method gives a C---I bond length closest to the G2(+) value, and only 0.072 Å and 0.088 Å shorter with the ECP/t and ECP/d basis sets, respectively. The difference with G2(+) theory, for the C---I bond length, is largest for the OPBE functional.

The geometry of the transition state was calculated previously with MP2/PTZ+ theory.<sup>83</sup> The structural difference between our calculations and MP2/PTZ+ mainly lies in the Cl–C bond length. The MP2/PTZ+ value is 2.350 Å, with which MP2/ECP/t gives the best agreement and only differs by 0.024 Å. HCTH407 theory gives the largest difference, with the MP2/PTZ+ TS Cl–C bond length, for both the ECP/d and ECP/t basis sets.

**B. Vibrational Frequencies.** Vibrational frequencies were calculated for all the stationary points by using the MP2 and DFT theories with both the ECP/d and ECP/t basis sets, and the results are listed in Table 2. These calculations were used to compare MP2 and DFT frequencies, and to compare them with experiments and other theoretical calculations. The frequencies calculated at the MP2 and MP2(fc) theories are quite consistent with the largest difference of 37  $\text{cm}^{-1}$  (out-of-plane bend of  $[\text{Cl--CH}_3\text{--I}]^-$ ) with the ECP/d basis and 51  $\text{cm}^{-1}$  ( $\text{A}_1$  C–H stretch of  $\text{Cl}^- \text{---CH}_3\text{I}$ ) with the ECP/t basis. The calculated frequencies of the  $\text{CH}_3\text{I}$  reactant and  $\text{CH}_3\text{Cl}$  product at the different levels of theory agree very well with experiment.<sup>88</sup> For the ECP/d basis, the average deviation is 1%, 2%, 3%, 1%, 2%, and 2% at the MP2, OPBE, OLYP, BhandH, HCTH407, and B97-1 theories, respectively. For the ECP/t basis the average deviation is 3%, 1%, 2%, 2%, 1%, and 1%, respectively.

The ECP/d and ECP/t basis sets give similar vibrational frequencies, with a largest difference of 54  $\text{cm}^{-1}$  ( $\text{A}_1$  C–H stretch of  $\text{CH}_3\text{I}$ ) for MP2, 31  $\text{cm}^{-1}$  (E  $\text{CH}_3$  deform of  $\text{Cl}^- \text{---CH}_3\text{I}$ ) for OPBE, 35  $\text{cm}^{-1}$  (E  $\text{CH}_3$  deform of  $\text{CH}_3\text{I}$ ) for OLYP, 56  $\text{cm}^{-1}$  ( $\text{A}_1$  C–H stretch of  $\text{CH}_3\text{I}$ ) for BhandH, 39  $\text{cm}^{-1}$  ( $\text{A}_1$   $\text{CH}_3$  deform of  $\text{Cl}^- \text{---CH}_3\text{I}$ ) for HCTH407, and 43  $\text{cm}^{-1}$  (E  $\text{CH}_3$  deform of  $\text{Cl}^- \text{---CH}_3\text{I}$ ) for B97-1, respectively. In general, the MP2 and DFT frequencies are in quite good agreement. However, a notable exception is the larger MP2 value for the imaginary reaction coordinate frequency as compared to the DFT functional values. With the ECP/t basis set the relative MP2:BhandH:OPBE:B97-1:HCTH407:OLYP values for this imaginary frequency are 1.59:1.26:1.07:1.07:1.03:1.00 and with the ECP/d basis set the relative values are 1.50:1.26:1.09:1.06:1.00:1.00. That the MP2 value for this frequency is substantially larger than the DFT values illustrates that the MP2 and DFT theories have different potential energy surface shapes in the vicinity of the  $[\text{Cl--CH}_3\text{--I}]^-$  central barrier.

There are several interesting effects concerning the frequencies calculated for  $\text{CH}_3\text{I}$  and  $\text{CH}_3\text{Cl}$  with the ECP/d and ECP/t basis sets and the MP2 and DFT theories. For the C–I and C–Cl stretches the ECP/t basis gives higher frequencies when used with both MP2 and DFT, consistent with the shorter bond lengths found with ECP/t as compared to ECP/d. Higher C–H stretch frequencies with ECP/t are also found for MP2, but not for DFT. Though the C–H bond distances are shorter when using ECP/t instead of ECP/d, for both MP2 and DFT, for DFT the ECP/t *E*-symmetry C–H stretch frequencies are significantly smaller than the ECP/d values. This same opposite trend for DFT, as compared to MP2 when using the ECP/d and ECP/t basis sets, is seen for the *E*-symmetry C–H stretch frequencies of the complexes and the central barrier.

Frequencies for  $\text{CH}_3\text{I}$ ,  $\text{CH}_3\text{Cl}$ , and the transition state  $[\text{Cl--CH}_3\text{--I}]^-$  have been calculated at the MP2/PTZ+ level.<sup>83</sup> The largest difference between the frequencies of MP2/ECP/t and those of MP2/PTZ+ is for the  $\text{A}_1$  C–H stretch of  $\text{CH}_3\text{I}$ , for which the MP2/ECP/t value is 49  $\text{cm}^{-1}$  larger. The principal difference between the frequencies of the DFT/ECP/t methods and those given by MP2/PTZ+ lies in the central barrier's imaginary frequency, and similar to the difference discussed above between MP2 and the DFT methods. The MP2/PTZ+ value for this frequency is 474i  $\text{cm}^{-1}$ . The ratio of this frequency divided by a DFT value ranges from 1.22 (BhandH) to 1.54 (OLYP). Since the two theories are fundamentally the same, MP2/ECP/t gives the best agreement with the MP2/PTZ+ calculations.

**C. Energies. 1. MP2 and DFT Energies.** MP2 and DFT electronic structure energies, for stationary points on the  $\text{Cl}^- + \text{CH}_3\text{I} \rightarrow \text{CH}_3\text{Cl} + \text{I}^-$  PES, are listed in Table 3. Though MP2 with the ECP/6-31+G(d) basis set method gives energies for  $\text{Cl}^- \text{---CH}_3\text{I}$  and  $[\text{Cl--CH}_3\text{--I}]^-$  similar to those obtained with the larger basis sets, this smaller basis set gives energies for  $\text{ClCH}_3\text{---I}^-$  and  $\text{CH}_3\text{Cl} + \text{I}^-$  much lower than those determined with the larger basis sets and is not considered further. There are differences in the MP2 energies calculated with and without the frozen core (fc) approximation. For the ECP/d basis these differences range from 0.3 to 0.9 kcal/mol and from 0.1 to 1.3 kcal/mol for the ECP/t basis. For both the MP2 and DFT calculations, the stationary point energies with the ECP/t basis are higher than those with the ECP/d basis. The size of this difference depends on the stationary point, and it ranges from 0.5–0.7, 1.2–2.3, 0.9–1.9, and 0.6–2.5 kcal/mol for  $\text{Cl}^- \text{---CH}_3\text{I}$ ,  $[\text{Cl--CH}_3\text{--I}]^-$ ,  $\text{ClCH}_3\text{---I}^-$ , and  $\text{CH}_3\text{Cl} + \text{I}^-$ , respectively. The differences between the ECP/d and ECP/t energies are most pronounced for MP2.

The different theories and ECP/d and ECP/t basis sets give quite a range of energies for each stationary point, which are 4.0, 5.9, 7.0, and 5.8 kcal/mol for  $\text{Cl}^- \text{---CH}_3\text{I}$ ,  $[\text{Cl--CH}_3\text{--I}]^-$ ,  $\text{ClCH}_3\text{---I}^-$ , and  $\text{CH}_3\text{Cl} + \text{I}^-$ , respectively. A reference for the stationary point energies was determined by performing high-level CCSD(T) calculations, as discussed in the next section.

**2. CCSD(T) Energies.** CCSD(T) calculations, based on the MP2/PP/d optimized geometries, were performed with the PP/d, PP/t, PP/q, and PP/5 basis sets and the resulting energies are listed in Table 4. These energies were extrapolated to the complete basis set (CBS) limit by using the formula proposed by Peterson et al.<sup>85</sup>

$$E(n) = E_{\text{CBS}} + A \exp[-(n-1)] + B_{\text{exp}}[-(n-1)^2] \quad (2)$$

where  $n = 2, 3, 4$ , and 5 representing the PP/d, PP/t, PP/q, and PP/5 basis sets. The CBS energies are also included in Table 4. The CCSD(T)/CBS energies for  $\text{Cl}^- \text{---CH}_3\text{I}$ ,  $[\text{Cl--CH}_3\text{--I}]^-$ ,

$\text{ClCH}_3\text{---I}^-$ , and products are  $\sim 0$ , 0.1, 0.3, and 0.3 kcal/mol lower than the CCSD(T)/PP/5 values, respectively, which shows good convergence toward the complete basis set limit for the CCSD(T) energies.

The resulting CCSD(T)/CBS energies are given in Figure 1 and listed in Table 3 where they are compared with the MP2 and DFT energies. The BhandH/ECP/t energies are in the best agreement with the CCSD(T)/CBS energies. The largest difference between these two sets of energies is 0.7 kcal/mol for the  $\text{Cl}^- \text{---} \text{CH}_3\text{I}$  complex and TS. For MP2, MP2/ECP/d gives the best agreement with the CCSD(T)/CBS energies with the largest difference of 2.5 kcal/mol for the products. The central barrier height calculated at OLYP/ECP/d theory is in the best agreement with the CCSD(T)/CBS value, with a small difference of 0.1 kcal/mol.

The role of ZPE on the stationary point energies is illustrated for the CCSD(T)/CBS calculations. The effect is small for  $\text{Cl}^- \text{---} \text{CH}_3\text{I}$  and  $[\text{Cl---CH}_3\text{---I}]^-$ , but almost 1 kcal/mol for  $\text{ClCH}_3\text{---I}^-$  and  $\text{CH}_3\text{Cl} + \text{I}^-$ , where the effect of including ZPE increases the stationary point energy. This latter effect results from the higher vibrational frequencies for the product  $\text{CH}_3\text{Cl}$ , as compared to the reactant  $\text{CH}_3\text{I}$ .

**3. Comparison with Experimental and Previous Theoretical Energies.** Energies for the stationary points have been determined from G2(+)<sup>54</sup> and MP2/PTZ+<sup>83</sup> ab initio calculations in previous studies. They are listed in Table 4, where they are compared with the CCSD(T) energies. With respect to the  $\text{Cl}^- + \text{CH}_3\text{I}$  reactants, G2(+) gives energies (zero-point energies are included) of  $-10.9$ ,  $-3.3$ ,  $-20.2$ , and  $-11.9$  kcal/mol for  $\text{Cl}^- \text{---} \text{CH}_3\text{I}$ ,  $[\text{Cl---CH}_3\text{---I}]^-$ ,  $\text{ClCH}_3\text{---I}^-$ , and  $\text{CH}_3\text{Cl} + \text{I}^-$ , respectively. For CCSD(T)/CBS these energies are  $-11.4$ ,  $-5.2$ ,  $-23.1$ , and  $-14.7$  kcal/mol. The largest difference between CCSD(T)/CBS and G2(+) energies is 2.9 kcal/mol for the  $\text{ClCH}_3\text{---I}^-$  complex. At the MP2(fc)/ECP/d level of theory, these energies are  $-11.4$ ,  $-3.9$ ,  $-20.6$ , and  $-11.4$  kcal/mol, and are in quite good agreement with the G2(+) energies, but are 1.3, 2.5, 3.3 kcal/mol more positive for the central barrier,  $\text{ClCH}_3\text{---I}^-$  complex, and products as compared to CCSD(T)/CBS. Similarly, the MP2/PTZ+ energies agree with the G2(+) values, but are more positive for the central barrier and products than the CCSD(T)/CBS values.

The complexation energies calculated here at the highest level of theory, i.e. CCSD(T)/CBS, are in agreement with those found from accurate HPMS experiments.<sup>89</sup> The classical complexation energies calculated for  $\text{Cl}^- \text{---} \text{CH}_3\text{I}$  and  $\text{I}^- \text{---} \text{CH}_3\text{Cl}$  are  $-11.5$  and  $-8.5$  kcal/mol. As shown in Table 4, including ZPE has only a small effect on these energies (i.e., 0.1 kcal/mol) and a small effect is also expected if a 298 thermal energy is included.<sup>53,54</sup> Complexation energies of  $\text{X}^- \text{---} \text{CH}_3\text{Y}$  complexes depend primarily on the identity of  $\text{X}^-$  and to a much smaller extent on the identity of  $\text{CH}_3\text{Y}$ .<sup>54</sup> Thus, the experimental complexation enthalpies,  $\Delta H_{\text{comp}}(298)$  for  $\text{Cl}^- \text{---} \text{CH}_3\text{Y}$  complexes, lie in a fairly narrow range.<sup>54,89</sup> The experimental  $\Delta H_{\text{comp}}(298)$  is  $-10.4$  and  $-12.5$  kcal/mol for  $\text{Cl}^- \text{---} \text{CH}_3\text{I}$  and  $\text{Cl}^- \text{---} \text{CH}_3\text{Br}$ , respectively. To convert these enthalpies to energies at 298 K, 0.6 kcal/mol is added, giving energies slightly less negative. The above CCSD(T)/CBS complexation energy for  $\text{Cl}^- \text{---} \text{CH}_3\text{I}$  is  $-11.5$  kcal/mol and quite consistent with the above experimental complexation energies. Though an experimental complexation enthalpy has not been reported for  $\text{I}^- \text{---} \text{CH}_3\text{Cl}$  an accurate HPMS value of  $\Delta H_{\text{comp}}(298) = -9.3$  kcal/mol has been reported for  $\text{I}^- \text{---} \text{CH}_3\text{I}$ , which is  $\sim 1$  kcal/mol more negative than the CCSD(T)/CBS classical complexation energy for  $\text{I}^- \text{---} \text{CH}_3\text{Cl}$ .

The experimental reaction exothermicity of  $-14.5$  kcal/mol,<sup>90</sup> listed in Table 4, is 1 kcal/mol more positive than the CCSD(T)/CBS value. The OPBE/ECP/d (Table 3) exothermicity is in the best agreement with the experimental exothermicity with a difference of 0.2 kcal/mol. The BhandH functional gives stationary point structures in good agreement with experiment and has a reaction exothermicity only 1.8 (ECP/d) and 1.3 (ECP/t) kcal/mol different than the experimental value (see Table 3).

Values of  $-2.7$  and  $-4.6$  kcal/mol for the  $[\text{Cl---CH}_3\text{---I}]^-$  central barrier height have been estimated by fitting the 300 K experimental rate constant using TST<sup>83</sup> and an ion–molecule capture statistical model.<sup>25</sup> However, the accuracy of these fits is somewhat uncertain given that experiments,<sup>23–31</sup> chemical dynamics simulations,<sup>32–50</sup> and quite-detailed statistical rate theory calculations<sup>91,92</sup> suggest that TST and statistical theories are not accurate models for  $\text{S}_{\text{N}}2$  reaction kinetics. However, it is worthwhile noting that, even if these models give rate constants in error by a factor of 10, this translates into only a 1.4 kcal/mol error in the barrier height! The expected effect of the TST and statistical model is to overestimate the  $\text{Cl}^- + \text{CH}_3\text{I}$  rate constant and, if this overestimation is a factor of 10, the actual barrier is then 1.4 kcal/mol lower than that deduced from the modeling. This would lower the estimated experimental central barrier heights to  $-4.1$  and  $-6.0$  kcal/mol, values quite consistent with the CCSD(T)/CBS barrier (Table 4). Thus, because of the above uncertainties in fitting the experimental rate constant it is difficult to deduce an accurate “experimental” central barrier height. A survey of all the electronic structure theory barrier heights, in Tables 3 and 4, indicates that the DFT/B97-1 central barrier may be too low.

#### IV. Summary

Extensive electronic structure calculations were performed for stationary points on the potential energy surface for the  $\text{Cl}^- + \text{CH}_3\text{I} \rightarrow \text{ClCH}_3 + \text{I}^-$   $\text{S}_{\text{N}}2$  nucleophilic substitution reaction to compare with experiment and to compare different electronic structure theories. The calculations were performed with the MP2 and CCSD(T) theories and the DFT functionals OPBE, OLYP, HCTH407, BhandH, and B97-1. For the MP2 and DFT calculations, the aug-cc-pVDZ and aug-cc-pVTZ basis sets<sup>82</sup> were used for the C, H, and Cl atoms and an effective core potential (ECP)<sup>80</sup> for the iodine atom. These basis sets are denoted as ECP/d and ECP/t, respectively. Single point energy calculations were performed at the CCSD(T) level of theory. The complete basis set (CBS) limit was extrapolated for the CCSD(T) calculations by using the aug-cc-pVXZ (X = D, T, Q, and 5) basis sets<sup>82</sup> for the C, H, and Cl atoms and a pseudopotential (PP)<sup>86</sup> for the iodine atom. These basis sets are identified as PP/x, x = d, t, q, and 5. In the following, the results obtained for the stationary point structures, vibrational frequencies, and energies are summarized. The MP2 calculations were performed with and without the frozen core (fc) approximation. The use of this approximation has only minor effects on the structures and frequencies, but alters the relative stationary point energies by as much as 1.3 kcal/mol. Differences between the MP2/ECP/d and MP2/PP/d stationary point geometries are quite small.

**A. Geometries.** Though the geometries obtained with the ECP/d and ECP/t basis sets are in good agreement for all the theories, ECP/t gives shorter bond lengths than ECP/d, except for the  $\text{Cl}^- \text{---} \text{C}$  and  $\text{C---I}^-$  bonds of the complexes. For these bonds, the DFT functionals give shorter bonds with ECP/d. DFT gives significantly longer halide ion/carbon atom bond lengths for the complexes than does MP2 theory. The geometries

obtained by BhandH/ECP/t theory give the best agreement with those determined with G2(+) theory<sup>54</sup> and the geometries obtained by MP2/ECP/t agree best with those from MP2/PTZ+ theory.<sup>83</sup> BhandH, with either the ECP/d or ECP/t basis set, gives the most accurate structures in comparison with experiment<sup>87</sup> when considering both  $\text{CH}_3\text{I}$  and  $\text{CH}_3\text{Cl}$ .

**B. Frequencies.** The frequencies calculated with ECP/d and ECP/t basis sets are in good agreement with differences less than  $56 \text{ cm}^{-1}$ . The major difference between the MP2 and DFT frequencies is for the imaginary frequency of the central barrier. By using the ECP/t basis the MP2 value for this frequency is 1.59 and 1.26 times larger than those given by the OLYP and BhandH functionals, respectively. Thus, the MP2 and DFT theories have different PES shapes in the vicinity of the  $[\text{Cl}^-\cdots\text{CH}_3\cdots\text{I}]^-$  central barrier. The frequencies of  $\text{CH}_3\text{I}$  and  $\text{CH}_3\text{Cl}$ , obtained at the different levels of theory and basis sets, are in excellent agreement with experiment<sup>88</sup> with differences ranging from 1% to 3%. For both MP2 and the DFT functionals, ECP/t gives shorter bond lengths for  $\text{CH}_3\text{I}$  and  $\text{CH}_3\text{Cl}$  than does ECP/d, and the trend is for ECP/t to give higher vibrational frequencies. The exception is for the DFT *E*-symmetry C–H stretch frequencies, which are lower for ECP/t as compared to ECP/d, even though the former gives shorter C–H bond lengths. In comparison with previous studies, the MP2/ECP/t frequencies are in the best agreement with those determined with MP2/PTZ+.<sup>83</sup>

**C. Energies.** Overall the energies obtained with the ECP/t basis set are slightly higher than those obtained with the ECP/d basis set for all the theories. CCSD(T)/CBS calculations were performed to determine approximate “benchmark” values for the stationary point energies, and the CCSD(T)/CBS results are in good agreement with experiments for the complexation energies<sup>89</sup> and reaction exothermicity.<sup>90</sup> For the latter energy, CCSD(T)/CBS is within 1 kcal/mol of experiment. The CCSD(T)/CBS value for the  $[\text{Cl}^-\cdots\text{CH}_3\cdots\text{I}]^-$  central barrier height is less than the value found by fitting the experimental  $\text{Cl}^- + \text{CH}_3\text{I} \rightarrow \text{ClCH}_3 + \text{I}^-$  rate constant with statistical theory,<sup>25,83</sup> which is consistent with the nonstatistical capture,<sup>44,93,94</sup> RRKM,<sup>33,39,93</sup> and barrier recrossing<sup>35,37,42</sup> dynamics<sup>3</sup> expected for this reaction. The BhandH energies are in overall best agreement with the CCSD(T)/CBS values, with a largest difference of only 0.7 kcal/mol for the ECP/t basis set. For MP2 theory the best agreement with the CCSD(T)/CBS energies is given by the MP2/ECP/d with the largest difference of 2.5 kcal/mol and for the products.

In summary, the work presented here has investigated the ability of different electronic structure theory methods to determine accurate stationary point properties for the  $\text{Cl}^- + \text{CH}_3\text{I} \rightarrow \text{ClCH}_3 + \text{I}^-$  PES. The results illustrate the ability of the higher level CCSD(T)/CBS theory to recover the experimental complexation enthalpies and reaction exothermicity. The more approximate MP2 theory and DFT functionals, which are practical for direct dynamics simulations<sup>51,95,96</sup> of the  $\text{Cl}^- + \text{CH}_3\text{I}$   $\text{S}_{\text{N}}2$  reaction, give different representations of its PES. At a high collision energy of 1.9 eV these methods give similar reaction dynamics, as has been reported,<sup>31</sup> but they give significantly different dynamics at lower collision energies.<sup>97</sup> The calculations reported here suggest that BhandH is the preferred method for direct dynamics simulations, since it gives reaction energies in the best agreement with the CCSD(T)/CBS values. The maximum difference is only 1.0 and 0.7 kcal/mol for the ECP/d and ECP/t basis sets, respectively. By using the ECP/d and ECP/t basis sets, a DFT direct dynamics calculation is 3 and 4 times faster, respectively, than one with MP2 and this, in itself, favors BhandH over MP2. The ECP/d basis set was used for the direct

dynamics simulation reported in ref 31, but use of the ECP/t basis set is also practical, since it only requires 5 and 7 times more computer time for BhandH and MP2 direct dynamics, respectively. It will be of interest to determine whether BhandH or another electronic structure theoretical method provides an accurate representation of the low collision energy dynamics for the  $\text{Cl}^- + \text{CH}_3\text{I} \rightarrow \text{ClCH}_3 + \text{I}^-$  reaction.

**Acknowledgment.** This material is based upon work supported by the National Science Foundation under Grant No. CHE-0615321 and the Robert A. Welch Foundation under Grant No. D-0005. Support was also provided by the High-Performance Computing Center (HPCC) at Texas Tech University, under the direction of Philip W. Smith. This research was performed in part using the Molecular Science Computing Facility (MSCF) in the William R. Wiley Environmental Molecular Sciences Laboratory, a national scientific user facility sponsored by the U.S. Department of Energy’s Office of Biological and Environmental Research and located at the Pacific Northwest National Laboratory, operated for the Department of Energy by Battelle. The authors wish to acknowledge important conversations with the Roland Wester research group, at the University of Freiburg, Germany, concerning dynamics of the  $\text{Cl}^- + \text{CH}_3\text{I}$   $\text{S}_{\text{N}}2$  nucleophilic substitution reaction.

## References and Notes

- (1) Farneth, W. E.; Brauman, J. I. *J. Am. Chem. Soc.* **1976**, *98*, 7891.
- (2) Moylan, C. R.; Brauman, J. I. In *Advances in Classical Trajectory Methods*; Hase, W. L., Ed.; JAI Press: New York, 1994; Vol. 2, p 95.
- (3) Hase, W. L. *Science* **1994**, *266*, 998.
- (4) Chabinyk, M. L.; Craig, S. L.; Regan, C. K.; Brauman, J. I. *Science* **1998**, *279*, 1982.
- (5) Angel, L. A.; Ervin, K. M. *J. Phys. Chem. A* **2004**, *108*, 9827.
- (6) DePuy, C. H.; Gronert, S.; Mullin, A.; Bierbaum, V. M. *J. Am. Chem. Soc.* **1990**, *112*, 8650.
- (7) Wladkowski, B. D.; Brauman, J. I. *J. Phys. Chem.* **1993**, *97*, 13158.
- (8) Shaik, S.; Ioffe, A.; Reddy, A. C.; Pross, A. *J. Am. Chem. Soc.* **1994**, *116*, 262.
- (9) Hase, W. L.; Cho, Y. J. *J. Chem. Phys.* **1993**, *98*, 8426.
- (10) Seeley, J. V.; Morris, R. A.; Viggiano, A. A.; Wang, H.; Hase, W. L. *J. Am. Chem. Soc.* **1997**, *119*, 577.
- (11) Bickelhaupt, F. M.; Buisman, G. J. H.; de Koning, L. J.; Nibbering, N. M. M.; Baerends, E. J. *J. Am. Chem. Soc.* **1995**, *117*, 9889.
- (12) Chandrasekhar, J.; Smith, S. F.; Jorgensen, W. L. *J. Am. Chem. Soc.* **1985**, *107*, 154.
- (13) Lieder, C. A.; Brauman, J. I. *J. Am. Chem. Soc.* **1974**, *96*, 4029.
- (14) Brauman, J. I.; Olmstead, W. N.; Lieder, C. A. *J. Am. Chem. Soc.* **1974**, *96*, 4030.
- (15) Olmstead, W. N.; Brauman, J. I. *J. Am. Chem. Soc.* **1977**, *99*, 4219.
- (16) Shaik, S.; Ioffe, A.; Reddy, A. C.; Pross, A. *J. Am. Chem. Soc.* **1994**, *116*, 262.
- (17) Dessent, D. E. H.; Johnson, M. A. *J. Am. Chem. Soc.* **1997**, *119*, 5067.
- (18) Ayotte, P.; Kim, J.; Kelley, J. A.; Johnson, M. A. *J. Am. Chem. Soc.* **1999**, *121*, 6950.
- (19) Su, T.; Chesnavich, W. J. *J. Chem. Phys.* **1982**, *76*, 5183.
- (20) Chesnavich, W. J.; Su, T.; Bowers, M. T. *J. Chem. Phys.* **1980**, *72*, 2641.
- (21) Baer, T.; Hase, W. L. In *Unimolecular Reaction Dynamics-Theory and Experiments*; Oxford: New York, 1996.
- (22) Glasstone, S.; Laidler, K. J.; Eyring, H. In *The Theory of Rate Processes*; McGraw-Hill: New York, 1941.
- (23) Graul, S. T.; Bowers, M. T. *J. Am. Chem. Soc.* **1991**, *113*, 9696.
- (24) Viggiano, A. A.; Morris, R. A.; Paschkewitz, J. S.; Paulson, J. F. *J. Am. Chem. Soc.* **1992**, *114*, 10477.
- (25) Graul, S. T.; Bowers, M. T. *J. Am. Chem. Soc.* **1994**, *116*, 3875.
- (26) Li, C.; Ross, P.; Szulejko, J. E.; McMahon, T. B. *J. Am. Chem. Soc.* **1996**, *118*, 9360.
- (27) DeTuri, V. F.; Hintz, P. A.; Ervin, K. M. *J. Phys. Chem. A* **1997**, *101*, 5969.
- (28) Angel, L. A.; Ervin, K. M. *J. Am. Chem. Soc.* **2003**, *125*, 1014.
- (29) Craig, S. L.; Brauman, J. I. *J. Phys. Chem. A* **1997**, *101*, 4745.
- (30) Wester, R.; Bragg, A. E.; Davis, A. V.; Neumark, D. M. *J. Chem. Phys.* **2003**, *119*, 10032.



- (31) Mikosch, J.; Trippel, S.; Eichhorn, C.; Otto, R.; Lourderaj, U.; Zhang, J.-X.; Hase, W. L.; Weidemüller, M.; Wester, R. *Science* **2008**, *319*, 183.
- (32) Vande Linde, S. R.; Hase, W. L. *J. Am. Chem. Soc.* **1989**, *111*, 2349.
- (33) Vande Linde, S. R.; Hase, W. L. *J. Chem. Phys.* **1990**, *94*, 6148.
- (34) Vande Linde, S. R.; Hase, W. L. *J. Chem. Phys.* **1990**, *93*, 7942.
- (35) Cho, Y. J.; Vande Linde, S. R.; Zhu, L.; Hase, W. L. *J. Chem. Phys.* **1992**, *96*, 8275.
- (36) Hase, W. L.; Cho, Y. J. *J. Chem. Phys.* **1993**, *98*, 8426.
- (37) Wang, H.; Peshlherbe, G. H.; Hase, W. L. *J. Am. Chem. Soc.* **1994**, *116*, 9644.
- (38) Peshlherbe, G. H.; Wang, H.; Hase, W. L. *J. Am. Chem. Soc.* **1996**, *118*, 2257.
- (39) Peshlherbe, G. H.; Wang, H.; Hase, W. L. *J. Chem. Phys.* **1995**, *102*, 5626.
- (40) Mann, D. J.; Hase, W. L. *J. Chem. Phys.* **1998**, *102*, 6208.
- (41) Su, T.; Wang, H.; Hase, W. L. *J. Phys. Chem. A* **1998**, *102*, 9819.
- (42) Sun, L.; Hase, W. L.; Song, K. *J. Am. Chem. Soc.* **2001**, *123*, 5753.
- (43) Sun, L.; Song, K.; Hase, W. L. *Science* **2002**, *296*, 875.
- (44) Wang, Y.; Hase, W. L.; Wang, H. *J. Chem. Phys.* **2003**, *118*, 2688.
- (45) Basilevsky, M. V.; Ryabov, V. M. *Chem. Phys. Lett.* **1986**, *129*, 71.
- (46) Schmatz, S.; Clary, D. C. *J. Chem. Phys.* **1998**, *109*, 8200.
- (47) Schmatz, S.; Botschwina, P.; Hauschildt, J.; Schinke, R. *J. Chem. Phys.* **2002**, *117*, 9710.
- (48) Henning, C.; Schmatz, S. *J. Chem. Phys.* **2004**, *121*, 220.
- (49) Henning, C.; Schmatz, S. *J. Chem. Phys.* **2005**, *122*, 234307.
- (50) Henning, C.; Oswald, R. B.; Schmatz, S. *J. Phys. Chem. A* **2006**, *110*, 3071.
- (51) Bolton, K.; Hase, W. L.; Peshlherbe, G. H. *Multidimensional Molecular Dynamics Methods*; Thompson, D. L., Ed.; World Scientific Publishing, Inc.: London, 1998; pp 143–189.
- (52) López, J. G.; Vayner, G.; Lourderaj, U.; Addepalli, S. V.; Kato, S.; deJong, W. A.; Windus, T. L.; Hase, W. L. *J. Am. Chem. Soc.* **2007**, *129*, 9976.
- (53) Glukhovtsev, M. N.; Pross, A.; Radom, L. *J. Am. Chem. Soc.* **1995**, *117*, 2024.
- (54) Glukhovtsev, M. N.; Pross, A.; Radom, L. *J. Am. Chem. Soc.* **1996**, *118*, 6273.
- (55) Glukhovtsev, M. N.; Pross, A.; Bernhard Schlegel, H.; Bach, R. D.; Radom, L. *J. Am. Chem. Soc.* **1996**, *118*, 11258.
- (56) Deng, L.; Branchadell, V.; Ziegler, T. *J. Am. Chem. Soc.* **1994**, *116*, 10645.
- (57) Tucker, S. C.; Truhlar, D. G. *J. Am. Chem. Soc.* **1989**, *93*, 8183.
- (58) Bento, A. P.; Solà, M.; Bickelhaupt, F. M. *J. Comput. Chem.* **2005**, *26*, 1497.
- (59) Parthiban, S.; de Oliveira, G.; Martin, J. M. L. *J. Phys. Chem. A* **2001**, *105*, 895.
- (60) Gonzales, J. M.; Cox, R. S., III; Brown, S. T.; Allen, W. D.; Schaefer, H. F., III *J. Phys. Chem. A* **2001**, *105*, 11327.
- (61) Gonzales, J. M.; Allen, W. D.; Schaefer, H. F., III *J. Phys. Chem. A* **2005**, *109*, 10613.
- (62) Swart, M.; Solà, M.; Bickelhaupt, F. M. *J. Comput. Chem.* **2007**, *28*, 1551.
- (63) Tucker, S. C.; Truhlar, D. G. *J. Am. Chem. Soc.* **1990**, *112*, 3338.
- (64) Vande Linde, S. R.; Hase, W. L. *J. Phys. Chem.* **1990**, *94*, 2778.
- (65) Li, G.; Hase, W. L. *J. Am. Chem. Soc.* **1999**, *121*, 7124.
- (66) Wang, H.; Zhu, L.; Hase, W. L. *J. Phys. Chem. A* **1994**, *98*, 1608.
- (67) Wang, H.; Hase, W. L. *J. Am. Chem. Soc.* **1997**, *119*, 3093.
- (68) Botschwina, P.; Horn, M.; Seeger, S.; Oswald, R. *Ber. Bunsenges. Phys. Chem.*; Seeger, S. Dissertation, Curvillier Verlag, Göttingen, 1995.
- (69) Wladkowski, B. D.; Allen, W. D.; Brauman, J. I. *J. Phys. Chem.* **1994**, *98*, 13532.
- (70) Botschwina, P. *Theor. Chem. Acc.* **1998**, *99*, 425.
- (71) Borisov, Y. A.; Arcia, E. E.; Mielke, S. L.; Garrett, B. C.; Dunning, T. H., Jr. *J. Phys. Chem. A* **2001**, *105*, 7724.
- (72) (a) Bylaska, E. J.; de Jong, W. A.; Govind, N.; Kowalski, K.; Straatsma, T. P.; Valiev, M.; Wang, D.; Apra, E.; Windus, T. L.; Hammond, J.; Nichols, P.; Hirata, S.; Hackler, M. T.; Zhao, Y.; Fan, P.-D.; Harrison, R. J.; Dupuis, M.; Smith, D. M. A.; Nieplocha, J.; Tipparaju, V.; Krishnan, M.; Wu, Q.; Van Voorhis, T.; Auer, A. A.; Nooijen, M.; Brown, E.; Cisneros, G.; Fann, G. I.; Fruchtl, H.; Garza, J.; Hirao, K.; Kendall, R.; Nichols, J. A.; Tsemekhman, K.; Wolinski, K.; Anchell, J.; Bernholdt, D.; Borowski, P.; Clark, T.; Clerc, D.; Dachsel, H.; Deegan, M.; Dyall, K.; Elwood, D.; Glendening, E.; Gutowski, M.; Hess, A.; Jaffe, J.; Johnson, B.; Ju, J.; Kobayashi, R.; Kutteh, R.; Lin, Z.; Littlefield, R.; Long, X.; Meng, B.; Nakajima, T.; Niu, S.; Pollack, L.; Rosing, M.; Sandrone, G.; Stave, M.; Taylor, H.; Thomas, G.; van Lenthe, J.; Wong, A.; Zhang, Z. *NWChem*, A Computational Chemistry Package for Parallel Computers, Version 5.1, Pacific Northwest National Laboratory, Richland, Washington, 2007. (b) High Performance Computational Chemistry: An Overview of NWChem a Distributed Parallel Application: Kendall, R. A.; Apra, E.; Bernholdt, D. E.; Bylaska, E. J.; Dupuis, M.; Fann, G. I.; Harrison, R. J.; Ju, J.; Nichols, J. A.; Nieplocha, J.; Straatsma, T. P.; Windus, T. L.; Wong, A. T. *Comput. Phys. Commun.* **2000**, *128*, 260–283.
- (73) Hehre, W. J.; Radom, L.; Schleyer, P. v. R.; Pople, J. A. *Ab Initio Molecular Orbital Theory*; Wiley: New York, 1986.
- (74) Adams, G. F.; Bent, G. D.; Bartlett, R. J.; Purvis, G. D. In *Potential Energy Surfaces and Dynamics Calculations*; Truhlar, D. G., Ed.; Plenum: New York, 1981; p 133.
- (75) Koch, W.; Holthausen, M. C. *A Chemist's Guide to Density Functional Theory*; Wiley-VCH: Weinheim, Germany, 2000.
- (76) Parr, R. G.; Yang, W. *Density Functional Theory of Atoms and Molecules*; Oxford University Press: New York, 1989.
- (77) Dreizler, R.; Gross, E. *Density Functional Theory*; Plenum Press: New York, 1995.
- (78) Perdew, J. P.; Ruzsinszky, A.; Tao, J. M.; Staroverov, V. N.; Scuseria, G. E.; Csonka, G. I. *J. Chem. Phys.* **2005**, *123*, 062201.
- (79) (a) Ditchfield, R.; Hehre, W. J.; Pople, J. A. *J. Chem. Phys.* **1971**, *54*, 724. (b) Hehre, W. J.; Ditchfield, R.; Pople, J. A. *J. Chem. Phys.* **1972**, *56*, 2257. (c) Rassolov, V. A.; Pople, J. A.; Ratner, M. A.; Windus, T. L. *J. Chem. Phys.* **1998**, *109*, 1223.
- (80) Wadt, W. R.; Hay, P. J. *J. Chem. Phys.* **1985**, *82*, 284.
- (81) Hu, W.-P.; Truhlar, D. G. *J. Phys. Chem.* **1994**, *98*, 1049.
- (82) (a) Dunning, T. H., Jr. *J. Chem. Phys.* **1989**, *90*, 1007. (b) Woon, D. E.; Dunning, T. H., Jr. *J. Chem. Phys.* **1993**, *98*, 1358.
- (83) Hu, W.-P.; Truhlar, D. G. *J. Am. Chem. Soc.* **1995**, *117*, 10726.
- (84) Raghavachari, K.; Trucks, G. W.; Pople, J. A.; Headgordon, M. *Chem. Phys. Lett.* **1989**, *157*, 479.
- (85) Peterson, K. A.; Woon, D. E.; Dunning, T. H., Jr. *J. Chem. Phys.* **1994**, *100*, 7410.
- (86) Peterson, K. A.; Shepler, B. C.; Figgen, D.; Stoll, H. *J. Phys. Chem. A* **2006**, *110*, 13877.
- (87) Lide, D. R. In *CRC Handbook of Chemistry and Physics*, 86th ed.; CRC Press: Boca Raton, FL, 2005.
- (88) Duncan, J. L.; Allan, A.; McKean, D. C. *Mol. Phys.* **1970**, *18*, 289.
- (89) Li, C.; Ross, P.; Szulejko, J. E.; McMahon, T. B. *J. Am. Chem. Soc.* **1994**, *118*, 9360.
- (90) Gurvich, L. V.; Veys, I. V.; Alcock, C. B. *Thermodynamic Properties of Individual Substances*, 4th ed.; Hemisphere Publishing Corporation: New York, 1989; Vol. 1, Elements O, H (D, T), F, Cl, Br, I, He, Ne, Ar, Kr, Xe, Rn, S, N, P and Their Compounds, Parts 1–2.
- (91) Wang, H.; Hase, W. L. *J. Am. Chem. Soc.* **1995**, *117*, 9347.
- (92) Wang, H.; Hase, W. L. *J. Am. Chem. Soc.* **1997**, *119*, 3093.
- (93) Vande Linde, S. R.; Hase, W. L. *J. Chem. Phys.* **1990**, *93*, 7962.
- (94) Hase, W. L.; Cho, Y. J. *J. Chem. Phys.* **1993**, *98*, 8626.
- (95) Hase, W. L.; Song, K.; Gordon, M. *Comput. Sci. Eng.* **2003**, *5*, 36–44.
- (96) Sun, L.; Hase, W. L. *Rev. Comput. Chem.* **2003**, *19*, 79.
- (97) Zhang, J.-X.; Lourderaj, U.; Hase, W. L. Work in progress.